Solid−Solid Structural Transformations in Lennard-Jones Clusters: Accurate Simulations versus the Harmonic Superposition Approximation†

Vladimir A. Sharapov and Vladimir A. Mandelshtam*

Chemistry Department, University of California at Irvine, Irvine, California 92697

Received: April 15, 2007; In Final Form: June 7, 2007

We consider systems undergoing very-low-temperature solid−solid transitions associated with minima of similar energy but different symmetry, and separated by a high potential barrier. In such cases the well-known "broken-ergodicity'' problem is often difficult to overcome, even using the most advanced Monte Carlo (MC) techniques, including the replica exchange method (REM). The methodology that we develop in this paper is suitable for the above specified cases and is numerically accurate and efficient. It is based on a new MC move implemented within the REM framework, in which trial points are generated analytically using an auxiliary harmonic superposition system that mimics well the true system at low temperatures. Due to the new move, the low-temperature random walks are able to frequently switch the relevant potential energy funnels leading to an efficient sampling. Numerically accurate results are obtained for a number of Lennard-Jones clusters, including those that have so far been treated only by the harmonic superposition approximation (HSA). The latter is believed to provide good estimates for low-temperature equilibrium properties but is manifestly uncontrollable and is difficult to validate. The present results provide a good test for the HSA and demonstrate its reliability, particularly for estimation of the solid−solid transition temperatures in most cases considered.

Introduction

In the present paper we are concerned with the so-called "solid−solid'' structural transformations that generally occur in clusters, such as van der Waals clusters. Although we only consider Lennard-Jones (LJ) clusters, both the methodology that we develop and our conclusions can possibly be extended to a broad range of problems, from protein folding to condensed-phase structural transformations.

Despite its simple form, the LJ pair potential is often used to model atomic and molecular interactions in complex systems, such as van der Waals clusters. LJ clusters have also become a benchmark for developing and testing various numerical algorithms.

A systematic analysis of LJ clusters reveals that generic properties, such as the melting temperature or temperature of surface reconstruction (see, e.g., refs 1−3), change monotonically with size. However, rich size-specific behavior of LJ clusters arises at low temperatures because the global energy minimum is highly sensitive to cluster size. Well-known examples of this behavior include clusters with sizes $n = 38$, 75−77, 98, and 102−104.[2,4−11] In each of these cases, the highly symmetric nonicosahedral global minimum belongs to a narrow funnel of the potential energy surface (see the overview[12] describing a "potential energy funnel''). A high potential barrier separates this narrow funnel from an icosahedral funnel. Albeit energetically less favorable, the low-energy icosahedral structures have higher vibrational entropy and, consequently, become thermodynamically more favorable at some finite, but usually low temperatures.[2,8] The corresponding structural transformation is then characterized as a "solid−solid'' transition. Accurate numerical simulations of such phenomena are extremely challenging and have become possible only recently due to the efficiency of the replica exchange method (REM)[13,14] and to gradually increasing computer power, which permits extremely long Monte Carlo (MC) runs. Selected examples of such calculations can be found in refs 1, 3, 9, 10, and 16. However, despite some recent successes, it is not hard to find a case that causes the standard version of the REM to display the "broken-ergodicity'' behavior.

Let K be the total number of replicas at temperatures $T_1 < T_2 < ... < T_K$. The sampling efficiency in the REM calculation at the lowest temperature, $T_{min} = T_1$, depends on exchanges with higher-temperature replicas, which can in turn exchange with even higher-temperature replicas. For sufficiently large $T_{max} = T_K$ these exchanges eventually allow the low-temperature replicas to travel between the physically relevant regions (funnels) of the configuration space. However, to switch funnels, the configurations of low-temperature replicas must climb the ladder of temperatures and reach sufficiently high replicas, where the original configurations can be replaced with configurations from other funnels. Consequently, one factor that makes the correlation times (i.e., the times associated with such a travel) very long is the height of the energy barrier separating the funnels. If the barrier is very high, the value of T_{max}, at which the system becomes ergodic, must be very high as well. Though the system is ergodic at high enough T_{max}, the system may still need very long times to find all the relevant funnel(s). Furthermore, to maintain equal exchange rates (e.g., 50%) between adjacent replicas for a fixed value of T_{max}, the required total number of replicas should grow approximately as $K \sim T_{min}^{-1}$.[17] This factor too can affect the correlation times significantly, because a very small value of T_{min} results in a large number of replicas.

Figure 1 gives an example of a system (the LJ_{31} cluster) that undergoes a low-temperature structural transformation from the

† Part of the special issue "Robert E. Wyatt Festschrift".

10.1021/jp072929c CCC: $37.00
Published on Web 08/09/2007

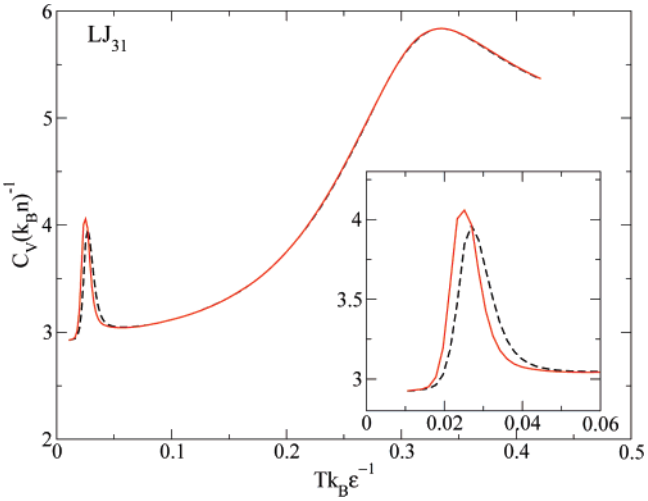

Figure 1. Low-temperature heat capacity for the LJ_{31} cluster from two independent REM calculations, in the absence of exchanges with the proposed auxiliary harmonic superposition system. In each calculation, averaging was over 1.5×10^9 MC steps, but the convergence of the low-temperature peak is still not perfect.

Mackay global energy minimum to the lowest anti-Mackay minimum.[3,18] The heat capacity was calculated with a standard version of the REM. Although a rigorous correlation time analysis has never been performed for this case, the lower-temperature peak shows noticeable differences between the two independent calculations, each using as many as 1.5×10^9 MC steps, where we define an MC step as one attempt to move a single particle in all the Metropolis random walks. (To reduce the statistical errors to the thickness of the curve, about 10^{10} MC steps are needed.) We note also that the case of LJ_{31} is relatively easy: because both low-temperature structures are of the same (icosahedral) type, the energy barrier separating those structures is not too high. The situation becomes much worse for LJ_{38},[9] where the random walks have to be an order of magnitude longer.

Recently, ref 10 reported heat capacities using the REM for LJ_{75-77} clusters. The simulations involved an order of 10^{11} MC steps per temperature, which is around the practical limit of currently available computers. The results seemed to converge based on the observation of stationary behavior starting after about 10^{10} equilibration steps. It is only the present methodology that allowed us to confirm the opposite (see below). An apparent stationarity that may be the case for a particular MC simulation, even if it occurs over extremely long times, is not sufficient to conclude that the convergence has been achieved!

The LJ clusters with sizes $n = 98$, and 102−104 represent even more pathological situations, for which the solid−solid transition temperatures are lower, whereas the potential barriers separating the competing funnels are higher. For these cases it is unlikely that the standard version of the REM can ever produce converged results.

Since the REM was introduced, numerous modifications of this method have been suggested. Some of these modifications combine the REM with the multicanonical algorithm (MUC),[2,19−21] and others combine the REM with simulated tempering (ST).[22] Generally, the idea is to use replicas with MUC or ST weight factors to make the exchanges more efficient, thus reducing the total number of replicas. The MUC factors can be obtained via recursive MC calculation,[23] or using multiple-histogram reweighting techniques[24] for data obtained from a short REM calculation,[25] or by Wang−Landau sampling.[26] Another way to improve sampling in comparison with the original REM is introduced in the so-called multidimensional REM (MREM),[27−29] which uses multiple swapping variables based on the idea that some replicas involved in the exchanges may have different Hamiltonians. Notable are also three recent proposals using the basin-sampling,[11] path-sampling[30] and the "min-map" method.[31] All the latter techniques attempt to design a general framework for overcoming the problem of adequate sampling of local energy minima separated by high barriers. The method that we develop in this paper is in many aspects very similar to yet another recent method called "smart darting with parallel tempering using the Eckart space'',[32] which is an improvement of the earlier idea of ref 33. In the smart darting method one attempts to make direct global moves from one energy minimum to prespecified set of other minima. However, even with the improvement of ref 32 the problem of having vanishingly low acceptance probabilities for the darting moves seem to be hard to overcome.

Method

Our proposal to overcome the broken-ergodicity problem, still within the REM framework, is to add to the set of conventional Metropolis random walks an auxiliary random walk that can switch often between two or more funnels. For a given set of energy minima, we consider an effective potential arising from the superposition of harmonic potentials approximating the true potential in the vicinity of each minimum. The use of such potential allows us to generate independent, canonically distributed random points analytically, thus minimizing the correlation times in the auxiliary system. To the best of our knowledge, this latter component of our method is new, whereas the idea of introducing an auxiliary system with better sampling properties and able to exchange its configurations with the system of interest is well-known. Note also, that the present methodology can be characterized as a version of the Metropolis−Hastings procedure using an "independence sampler''. A well-known example of the use of an independence sampler is the J-walking algorithm,[34] in which (approximately) independent samples are generated by a Metropolis random walk at a high temperature, taking configurations that are sufficiently far apart from each other. Here the independence sampler takes truly independent configurations from the Gaussian superposition.

We consider an n-atom system described by the potential $V(\mathbf{r})$ using the mass-scaled ($r_i \rightarrow \sqrt{m_i} r_i$) Cartesian coordinates $\mathbf{r} \in \mathbb{R}^{3n}$, represented as column vectors:

$$\mathbf{r} = \begin{pmatrix} r_1 \\ \vdots \\ r_n \end{pmatrix} \qquad r_i = \begin{pmatrix} x_i \\ y_i \\ z_i \end{pmatrix} \tag{1}$$

Without loss of generality we only consider configurations with the center of mass located at zero:

$$\sum_{i=1}^{n} \sqrt{m_i} r_i = 0 \tag{2}$$

where m_i define the atomic masses and r_i, the mass-scaled position vectors.

Let $\{\mathbf{r}_\alpha\}$ ($\alpha = 1, ..., L$) be configurations of L different energy minima that are separated by high barriers and are assumed to contribute to the properties of the system at low temperatures. Formulation of the present method would be straightforward if the energy minima were points in the configuration space. Unfortunately, for a cluster the situation is complicated because $V(\mathbf{r})$ is invariant not only under translations, inversion, and

permutations of atoms but also under rotations of the cluster around its center of mass. Factoring out the translations, every minimum gives rise to $2\prod_k n_k!/h_\alpha$ of 3-dimensional manifolds, where h_α is the order of the point group for the α-th minimum, and n_k defines the number of atoms of the kth type.

Strictly speaking, the $3n$-dimensional Gaussian distribution arising from the harmonic approximation is not a meaningful approximation to the true low-temperature canonical distribution and is not even defined uniquely. The latter is because the harmonic potential, unlike the true potential, is not invariant under rotations. In what follows we give an unambiguous definition of the harmonic superposition system, which has the same symmetries as the true system.

For each minimum, let K_α be the $3n \times 3n$ mass-scaled Hessian, with 3×3 blocks defined by

$$K_{\alpha ij} = \frac{\partial^2 V(\mathbf{r})}{\partial r_i \partial r_j} \tag{3}$$

K_α has exactly six zero eigenvalues, three resulting from the invariance of $V(\mathbf{r})$ with respect to the translations of the center of mass and three, to rotations of the whole cluster around the origin (i.e, its center of mass). When stacked together, the three rotational eigenvectors of K_α form the $3 \times 3n$ matrix

$$Q_\alpha = \begin{pmatrix} Q_{\alpha 1} \\ \vdots \\ Q_{\alpha n} \end{pmatrix} \tag{4}$$

where the 3×3 matrices $Q_{\alpha i}$ ($i = 1, ..., n$) are given in terms of the components of $\mathbf{r}_\alpha$:

$$Q_{\alpha i} = \begin{pmatrix} 0 & -z_{\alpha i} & y_{\alpha i} \\ z_{\alpha i} & 0 & -x_{\alpha i} \\ -y_{\alpha i} & x_{\alpha i} & 0 \end{pmatrix} \tag{5}$$

Let Ω_α be a disk of sufficiently small radius δ that belongs to the purely vibrational hyperplane, i.e., the $(3n - 6)$-dimensional hyperplane orthogonal to all the translational and rotational eigenvectors of K_α. That is,

$$\mathbf{r} \in \Omega_\alpha \quad \text{iff} \quad ||\mathbf{r} - \mathbf{r}_\alpha|| < \delta \quad \text{and} \quad Q_\alpha^{\mathrm{T}}\mathbf{r} = 0 \tag{6}$$

We note that $\mathbf{r}$ is automatically orthogonal to the translational eigenvectors of K_α due to the assumption of eq 2. Realizing the identity

$$Q_\alpha^{\mathrm{T}}\mathbf{r} = \sum_i r_{\alpha i} \times r_i \tag{7}$$

the conditions $\sum_i r_{\alpha i} \times r_i = 0$ and $\sum_i \sqrt{m_i} r_i = 0$ define the so-called Eckart space of configuration $\mathbf{r}_\alpha$,[35] which has been used in a very similar context in ref. 32 to account for cluster rotations in the framework of the Smart Darting algorithm.

For points $\mathbf{r} \in \Omega_\alpha$ the harmonic potential is defined as

$$V_\alpha(\mathbf{r}) = E_\alpha + \frac{1}{2}(\mathbf{r} - \mathbf{r}_\alpha)^{\mathrm{T}} K_\alpha (\mathbf{r} - \mathbf{r}_\alpha) \tag{8}$$

together with the normalized Gaussian distribution

$$G_\alpha(\mathbf{r};\beta) = \frac{1}{Z_\alpha(\beta)} e^{-\beta V_\alpha(\mathbf{r})} \tag{9}$$

Here the vibrational partition function for the αth minimum is

$$Z_\alpha(\beta) = \mathrm{e}^{-\beta E_\alpha}\left(\frac{\beta}{2\pi}\prod_{i=1}^{3n-6}\lambda_{\alpha i}\right)^{-1/2} \tag{10}$$

with the product taken over the nonzero eigenvalues, $\lambda_{\alpha i}$, of K_α.

Note again that the reduced harmonic superposition system defined by eqs 8 and 9 (as originally introduced in ref 36) is not yet invariant with respect to the rotations and permutations. Although this property is irrelevant for the harmonic superposition approximation (HSA),[36] it is required here.

For a point r in the vicinity of one of the minima define its projection

$$\mathbf{r}_\Omega := \mathscr{R}\mathscr{P}\mathbf{r} \in \Omega_\alpha \tag{11}$$

where $\mathscr{P}$ is an appropriate permutation of the atoms and $\mathscr{R}$ is a rotation (possibly including the inversion) of the cluster around the origin. An algorithm of finding such $\mathscr{P}$ and $\mathscr{R}$ is described in the Appendix. The latter turned out to be nearly identical to that in ref 32. We can now extend the definition of the harmonic potential to the subset that can be generated from Ω_α by the inversion and all possible rotations and permutations:

$$V_{\mathrm{harm}}(\mathbf{r}) := V_\alpha(\mathbf{r}_\Omega) \tag{12}$$

Consequently, we define the canonical distribution function for the extended harmonic superposition system:

$$G(\mathbf{r};\beta) \sim e^{-\beta V_{\mathrm{harm}}(\mathbf{r})} \tag{13}$$

Unlike the reduced superposition system, the extended system defined by eqs 12 and 13 is invariant under the same symmetry operations as the true physical system. In particular, at sufficiently large values of the inverse temperature $\beta = 1/k_{\mathrm{B}}T$, eq 13 mimics the true Boltzmann distribution,

$$W(\mathbf{r};\beta) \sim \mathrm{e}^{-\beta V(\mathbf{r})} \tag{14}$$

Most importantly, random points distributed according to $G(r;\beta)$ can be generated analytically, as the latter can be represented as a superposition of normalized Gaussian distributions. To correctly account for permutation and rotation/inversion symmetries, we generate the random points only within the set $\Omega := \cup_\alpha \Omega_\alpha$ with the reduced distribution function

$$G_\Omega(\mathbf{r};\beta) = \sum_\alpha P_\alpha(\beta)\, G_\alpha(\mathbf{r};\beta) \qquad \mathbf{r} \in \Omega \tag{15}$$

where the weights are

$$P_\alpha(\beta) = \frac{1}{Z(\beta)}\frac{Z_\alpha(\beta)}{h_\alpha} \qquad Z(\beta) = \sum_\alpha \frac{Z_\alpha(\beta)}{h_\alpha} \tag{16}$$

For sufficiently large values of β the Gaussians practically vanish outside the disks Ω_α, so we have the normalization conditions

$$\int_{\Omega_\alpha} G_\alpha(\mathbf{r};\beta)\, \mathrm{d}\mathbf{r} = 1 \qquad \sum_\alpha P_\alpha(\beta) = 1 \tag{17}$$

The two probability distributions (eqs 13 and 15) are related as

$$\frac{\int_{\mathbb{R}^{3n}} F(\mathbf{r})\, G(\mathbf{r};\beta)\, \mathrm{d}\mathbf{r}}{\int_{\mathbb{R}^{3n}} G(\mathbf{r};\beta)\, \mathrm{d}\mathbf{r}} = \frac{\int_\Omega F(\mathbf{r})\, G_\Omega(\mathbf{r};\beta)\, \mathrm{d}\mathbf{r}}{\int_\Omega G_\Omega(\mathbf{r};\beta)\, \mathrm{d}\mathbf{r}} \tag{18}$$

for any function $F(\mathbf{r})$ that is invariant to translations, rotations, inversion, and permutations of identical atoms. This means that, within the harmonic superposition framework,[36] computation of such properties only requires averaging over the reduced set Ω. In the cases when the property of interest is not invariant with respect to the said symmetries, one needs to use the extended distribution function $G(\mathbf{r};\beta)$. Once a random point distributed according to the reduced distribution $G_\Omega(\mathbf{r};\beta)$ can be generated within set Ω, a point in $\mathbb{R}^{3n}$ distributed according to $G(\mathbf{r};\beta)$ can also be generated from this point by a random rotation/inversion followed by a random permutation.

We now consider a set of coupled random walks running at different temperatures according to the standard REM scheme,[13,14] which maintains the Boltzmann probability distribution (14) in each random walk. Such a scheme includes at least two types of moves, namely, a standard Metropolis move involving a single random walk, and a move involving exchanges of configurations between two random walks with similar temperatures. *The new move* can be interpreted as configuration exchange between a particular random walk and the auxiliary harmonic superposition system, although the random configurations of the auxiliary system are independent. The implementation of the new move involves analytic generation of a random trial point $\mathbf{r}' \in \Omega$ according to the probability distribution (15). (As described above, if needed, a random point $r' \in \mathbb{R}^{3n}$ with distribution $G(r;\beta)$ can also be generated.) The trial point is then accepted with probability

$$P(\mathbf{r}\rightarrow\mathbf{r}') = \min\left\{1, \frac{W(\mathbf{r}';\beta)\, G(\mathbf{r};\beta)}{W(\mathbf{r};\beta)\, G(\mathbf{r}';\beta)}\right\} = \min\{1, e^{\beta[\Delta V(\mathbf{r}')-\Delta V(\mathbf{r})]}\} \quad (19)$$

where $\Delta V(\mathbf{r}) = V_{\mathrm{harm}}(\mathbf{r}) - V(\mathbf{r})$. Clearly, the number of minima in the auxiliary system can be greater than 2 and the new move can be utilized independently for different random walks running at different temperatures.

The new move (as well as the standard REM moves) satisfies the detailed balance condition, which ensures that the points in the random walks generated by such moves will be distributed according to $W(\mathbf{r};\beta)$. Furthermore, the new move is to be implemented only for particular random walk(s), for which the switching rate is significant. Exchanges of configurations between the coupled random walks maintain ergodicity of the system at all temperatures.

The sampling efficiency of the new move depends on how frequently the random walk switches from one minimum to another. The switching rate in turn depends on the following two factors.

(i) The probabilities, $P_\alpha(\beta)$, for the trial point $\mathbf{r}'$ to appear in different minima. This factor can be optimized by adjusting the value of β. For example, equal statistical weights ($P_1(\beta) = P_2(\beta)$) for two selected minima correspond to the value[2]

$$\beta_{\mathrm{HSA}} = \frac{\frac{1}{2}\sum_i \ln(\lambda_{1i}/\lambda_{2i}) + \ln(h_1/h_2)}{E_2 - E_1} \quad (20)$$

(ii) How well the harmonic potential approximates the true potential for points sampled by the canonical distribution at $\beta = \beta_{\mathrm{HSA}}$. The acceptance probability (19) will have an appreciable value when $V(\mathbf{r})$ is not very different from $V_{\mathrm{harm}}(\mathbf{r})$, i.e., when $\Delta V(\mathbf{r})$ is small. However, when the harmonic approximation is poor, regardless of the other factors, $P(\mathbf{r}\rightarrow\mathbf{r}')$ will be nearly zero. For example, the harmonic approximation is very good for LJ_n clusters with $n = 31, 98, 102-104$ at temperatures of the corresponding solid−solid transitions. For these clusters the switching rates are between 0.01 and 0.1. For $n = 38, 75$ the harmonic approximation is not very good, resulting in switching rates of 5×10^{-4} and 5×10^{-3}, respectively. Fortunately, for the latter two cases the seemingly low switching rates are still sufficient to provide adequate numbers of exchanges between the relevant funnels for simulations using an order of 10^9 MC steps.

Expression 20 is known in the context of the HSA.[2,36] As long as the potential energy is "well'' represented by its harmonic approximation for the corresponding energy range, eq 20 provides a good estimate for the temperature of the structural transformation from one minimum to the other. Consequently, the HSA becomes more accurate for cases with lower transition temperatures. One should realize though that even when the harmonic approximation is poor to maintain appreciable switching rates between different funnels, it may still be adequate for estimating the heat capacity near the transition temperature, and possibly vice versa. Note also that, given $E_1 < E_2$, eq 20 will give a positive value of β_{HSA} only if the numerator is negative, i.e., when the vibrational-configurational entropy of the higher-energy minimum is greater than that of the lower-energy minimum. This may happen particularly for certain "magic-number'' LJ clusters with nonicosahedral global minima.[2]

Results and Discussion

In this section we apply our method to LJ_n clusters with $n = 31, 38, 75, 98, 102-104$. The part of all the replica-exchange calculations not associated with the *new move* used the methodology described in ref. 3. That is, for each cluster the replica temperatures T_k within the temperature interval of interest were chosen self-consistently using an adaptive procedure of ref 14 with the goal that the mean exchange rate between replicas with adjacent temperatures, T_k and T_{k+1}, would be about 50%, and remain approximately constant with k. The canonical averages between the replica temperatures ($T_k < T < T_{k+1}$) were interpolated using the following expression:[15]

$$\langle A\rangle_T \approx \alpha_k(T)\, A_k(T) + [1 - \alpha_k(T)]A_{k+1}(T) \quad (21)$$

where

$$\alpha_k(T) = \cos^2\left[\frac{\pi(T - T_k)}{2(T_{k+1} - T_k)}\right]$$

and

$$A_k(T) = \frac{1}{Z_k(T)}\sum_{m=1}^{N_{\mathrm{MC}}} \exp\left[\frac{(T - T_k)V(\mathbf{r}_m^{(k)})}{k_{\mathrm{B}}TT_k}\right]A(\mathbf{r}_m^{(k)})$$

$$Z_k(T) = \sum_{m=1}^{N_{\mathrm{MC}}} \exp\left[\frac{(T - T_k)V(\mathbf{r}_m^{(k)})}{k_{\mathrm{B}}TT_k}\right] \quad (22)$$

Here $\{\mathbf{r}_m^{(k)}\}$ ($m = 1, ..., N_{\mathrm{MC}}$) define canonically distributed random points at temperature T_k. As long as $\alpha_k(T)$ is a smooth function with $\alpha_k(T_k) = 1$ and $\alpha_k(T_{\{k+1\}}) = 0$, its choice is not important. Note that in principle eq 22 alone gives an exact expression for $\langle A\rangle_T$ for any T and T_k in the $N_{\mathrm{MC}} \rightarrow \infty$ limit. However, practically, it can be used only when the difference $T - T_k$ is not too large.

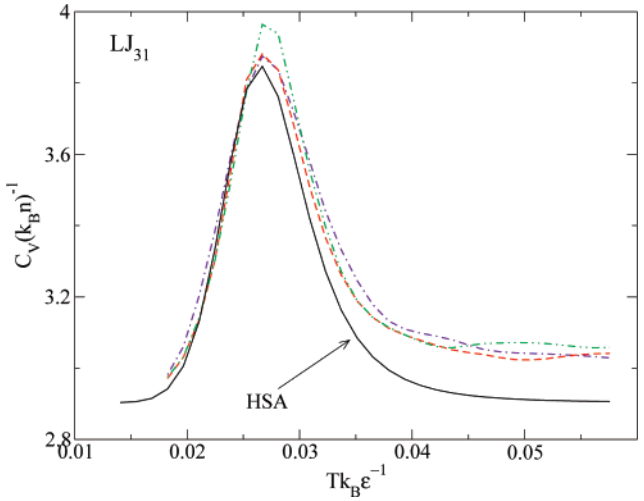

Figure 2. Low-temperature heat capacity for LJ_{31} cluster computed by the present method using three independent calculations. In each case the averaging was performed using 10^7 MC steps, which is a factor of 100 shorter than what was used in Figure 1. Also shown is the result of the HSA using only the two lowest energy minima.

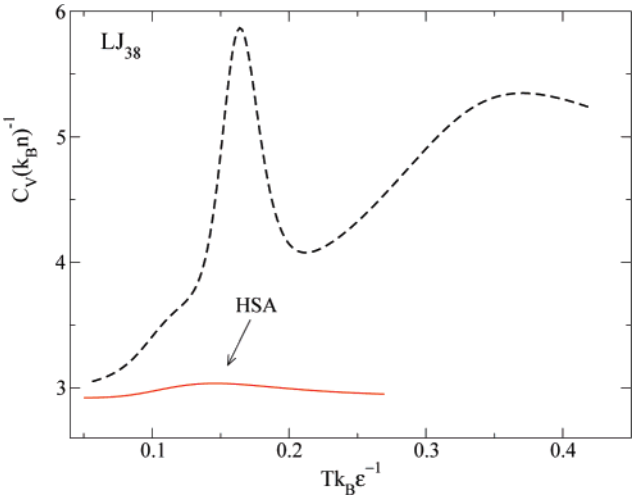

Figure 3. Heat capacity of the LJ_{38} cluster computed by the present method using 10^9 MC steps per temperature (the dashed curve). It is indistinguishable from that computed by the standard REM using 10^{10} MC steps. The shoulder around $T \sim 0.12$ is due to the solid−solid transition from the octahedral global minimum to the lowest icosahedral minimum. The HSA (the solid curve) using the two lowest minima results in a small peak around $T \sim 0.14$.

The simulations were performed using a hard constraining sphere with radius $R_c = 3\sigma$ for $n = 31$, 38, $R_c = 3.5\sigma$ for $n = 75$, and $R_c = 4\sigma$ for $n = 98$, 102−104. The swaps between each pair of adjacent replicas were attempted once per 100 local Metropolis moves.

For LJ_{31} and LJ_{38} clusters converged heat capacities computed by the standard REM are available (see, e.g., refs 3 and 9). Therefore, these clusters are good benchmark systems for testing new computational methods. Consequently, the present method was applied to both systems to verify that the heat capacities computed by the new method are indistinguishable, within the statistical errors, from those computed by the standard version of the REM. (The comparisons are not shown here.)

The solid−solid transition in LJ_{31} occurs at $T = 0.027$ and is due to the competition between the Mackay global minimum and anti-Mackay local minima structures. Although more than two energy minima contribute to the low-temperature peak, our auxiliary harmonic superposition system included only two minima, one per funnel. The fact that we did not include all the local minima does not make our method approximate, while at the same time having the two minima still removes the numerical bottleneck associated with the slow switching rate between the two major funnels. Because for LJ_{31} the solid−solid transition temperature is relatively low, the harmonic approximation is good and so the switching rate between the Mackay and anti-Mackay funnels is of the order of 10 %.

Figure 2 shows the heat capacity of LJ_{31} computed by the present method using three independent calculations. In each calculation the averaging was performed over 10^7 MC steps, which is by a factor of 100 shorter than what was used in Figure 1, but, at the same time, results in even smaller statistical errors for the present method. That is, for the case of LJ_{31}, the numerical gain due to the exchanges with the harmonic superposition system turns out to be between 2 and 3 orders of magnitude compared to the regular REM calculation!

We also carried out a calculation in the temperature interval [0.015:0.05] using the four lowest minima, which according to the HSA are expected to give the main contribution to the equilibrium properties in this temperature range. The result turned out to be indistinguishable from that obtained by the conventional REM calculation using $\sim 10^{10}$ MC steps. Note that for this temperature interval the only mechanism that could make the simulation ergodic is the exchanges with the harmonic superposition system.

Figure 2 also shows the heat capacity of LJ_{31} estimated by the HSA

$$C_{V,\mathrm{HSA}}(T) = \frac{\partial}{\partial T}\left[k_B T^2 \frac{\partial \ln Z(\beta)}{\partial T}\right] \tag{23}$$

where $Z(\beta)$ is computed by eq 16 using the lowest two energy minima. Notably, $C_{V,\mathrm{HSA}}(T)$ agrees very well with the accurate simulation.

For the other well-studied case of LJ_{38} a converged heat capacity was first reported in ref 9. As was first recognized in ref 37, the thermodynamics of this system below the melting transition is due to the competition between the octahedral global minimum and icosahedral local minima structures that belong to two different funnels of the potential energy surface.[37] Because the solid−solid transition occurs close to the melting transition, it manifests itself in a small shoulder of the strong melting peak (see Figure 3). For LJ_{38}, as well as for LJ_{31}, the harmonic superposition system included only the two lowest minima (one per funnel). With these two minima, eq 20 gives $T_{\mathrm{HSA}} \sim 0.14$ for the temperature of the solid−solid transition. At this relatively high temperature the switching rate between the two funnels is around 5×10^{-4}, which is quite low. However, because such a switching rate is still much higher than that in a REM simulation alone, the number of MC steps required to obtain statistical errors less than the thickness of the curve in Figure 3 is about 10^9, which gives about an order of magnitude improvement compared to the standard REM.

In the next example we consider the LJ_{75} cluster, which has decahedral global minimum, with the solid−solid transition toward the lowest icosahedral minimum estimated to be at $T_{\mathrm{HSA}} = 0.082$ according to the HSA.[2] As in the previous examples the auxiliary system included only two lowest energy minima (one per funnel). The well-converged result using the present method with 3×10^9 MC steps is shown in Figure 4, where the statistical errors are estimated to be within the thickness of the heat capacity curve. The maximum occurs at $T = 0.083$, i.e., just slightly above the HSA estimate. The figure also shows the results from ref 10 using the standard version of REM. In

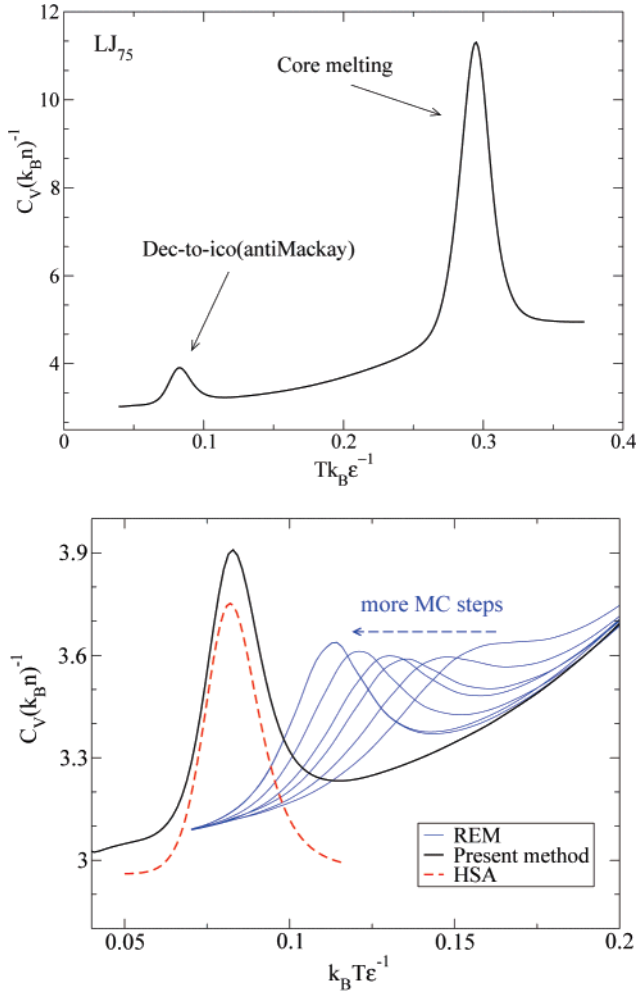

Figure 4. Upper panel: the numerically converged heat capacity of LJ_{75} cluster computed by the present method. For each of the two heat capacity peaks the type of the structural transformation is indicated. Lower panel: the heat capacity in the low-temperature regime is compared with that computed by two other methods. Each of the seven curves in the REM calculation has been computed by collecting averages for successive groups of 2×10^9 MC steps per temperature. The peak gradually shifts to the lower temperatures, but after about 10^{10} MC steps stops moving: the last two curves are hardly distinguishable on the plot. The latter also coincide with that obtained by collecting averages over 1.5×10^{10} MC steps after 10^{10} equilibration steps. It is tempting to conclude that the REM calculation is converged!

the latter simulation the global minimum configuration was used to initialize all the random walks. This explains why the solid−solid heat capacity peak evolves toward the lower temperatures with increasing number of equilibration steps. It though becomes stationary after about 10^{10} steps and its position with maximum at $T = 0.114$ remains the same even after $\sim 10^{11}$ MC steps. This apparent stationary behavior was mistakenly interpreted in ref 10 as evidence of convergence.

We also performed calculations for several other LJ_n ($n =$ 98, 102−104) clusters with nonicosahedral global minima. The global minimum of LJ_{98} has tetrahedral symmetry, and the global minima of $LJ_{102-104}$ have decahedral symmetry. The next-in-energy local minimum in each case is a Mackay icosahedron. So far the corresponding solid−solid structural transitions for these systems have been characterized only using the HSA.[2] In the present study, the replica temperatures were chosen to cover only the ranges around the low-temperature peak. This choice is possible because at sufficiently low temperatures only the two lowest energy minima make a noticeable contribution to

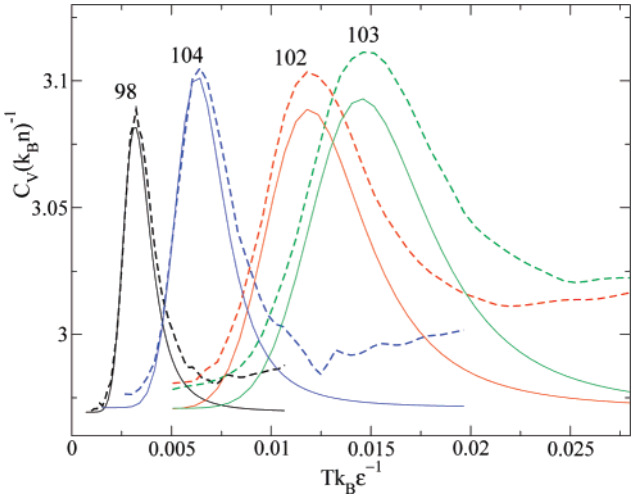

Figure 5. Heat capacities of LJ_n clusters with $n = 98$, 102−104, computed by the present method (dashed lines) and by the HSA (solid lines). In each case the peak is due to the solid−solid structural transition from the global nonicosahedral energy minimum to the lowest icosahedral local minimum.

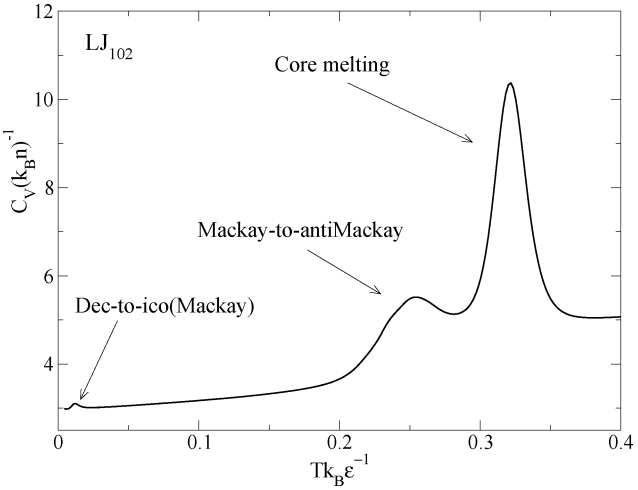

Figure 6. Heat capacity of LJ_{102} computed by the present method. The full $C_V(T)$ curve was obtained by pasting together the results from two independent calculations: one using the present method for temperatures $T < 0.03$, and the other, using the conventional REM for $T > 0.03$.[3] For each heat capacity peak the type of the structural transformation is indicated.

the properties of these systems. For each case we performed about 5×10^9 MC steps per temperature. The results are shown in Figure 5. Most interestingly, as in the previous examples the HSA gives an excellent estimate of the heat capacity at low temperatures, which is now confirmed numerically. At higher temperatures all clusters in this size range undergo two more structural transformations:[3] the Mackay-to-anti-Mackay surface reconstruction and core melting. This is shown in Figure 6 for LJ_{102}, for which the heat capacity has two other peaks at higher temperatures.

Finally, Table 1 summarizes our results on the temperatures of the solid−solid transition in the LJ clusters considered in this paper.

Conclusions

This paper presents a substantial improvement of the REM to accurately simulate very-low-temperature structural transformations in many-body systems and demonstrates its applicability to several LJ clusters, including those that seemed

TABLE 1: Temperature Estimates of the Solid−Solid Transitions in LJ_n Clusters Obtained by the HSA (Eq 20) Using the Lowest Two Minima and by the Present Method

n	harmonic superposition	present method
31	0.0264	0.0271
75	0.0820	0.0829
98	0.0032	0.0032
102	0.0119	0.0119
103	0.0145	0.0148
104	0.0063	0.0063

so far to be numerically intractable. Orders of magnitude improvements in terms of the computational times could be achieved for certain systems that undergo low-temperature structural transformations due to existence of at least two competing structural types.

In all cases that we considered (except, maybe, LJ_{38}) the HSA[36] provides a very accurate estimate for the low-temperature heat capacity around the solid−solid transition. The excellent agreement between the HSA and the simulations is somewhat surprising and may even seem disappointing due to the triviality of the harmonic analysis versus the complexity of the Monte Carlo simulations. However, the reliability of the HSA had become evident only after direct comparisons with numerically accurate results became possible, whereas without such comparisons the uncontrollable approximation provided by the HSA could always be questioned.

In principle, the method can also be applied in a similar context to other systems, e.g., to describe solid−solid phase transitions in bulk materials or equilibrium properties of proteins involving different conformations. However, the requirement of an a priori knowledge of the minima representing the relevant funnels may make the method difficult to apply, especially in the cases corresponding to excessively large numbers of local minima involved. Moreover, even when the relevant minima are known, the method may still be impractical if the transition temperatures between the minima (cf. eq 20) are too high: at high energies the harmonic approximation of the potential may be inadequate, resulting in turn in vanishingly small acceptance probabilities. One solution to this problem may be, for instance, an introduction of additional swapping parameters.

Another problem, which makes the present method involving the *new move* difficult to apply to large systems, is however consistent with the general property of the Monte Carlo methodology. Namely, the acceptance probabilities of moves involving global configuration changes tend to become exponentially small when the dimensionality of the system is increased, whereas the local moves could potentially have appreciable acceptance probabilities but are hard to design so that they could lead to efficient sampling of the whole configuration space.

Appendix: Identification and Matching of Similar Cluster Configurations

Given a configuration $\mathbf{r} = (r_1, ..., r_n)^T$ of an n-atom cluster that is presumably close to one of the reference configurations $\mathbf{r}_\alpha = (r_{\alpha 1}, ..., r_{\alpha n})^T$, we describe an algorithm for finding an appropriate permutation of identical atoms and rotation of the whole cluster around its center of mass (possibly including the inversion) that for the resulting configuration makes the norm $||\mathbf{r} - \mathbf{r}_\alpha||$ sufficiently small with condition (6) satisfied. The present algorithm turns out to be nearly identical to that used in ref 32.

Any two nonparallel vectors $r_1, r_2 \in \mathbb{R}^3$ define an orthonormal basis in $\mathbb{R}^3$ as

$$\begin{aligned} e_1 &= r_1/|r_1| \\ \tilde{e}_2 &= r_2 - e_1^T r_2 e_1 \\ e_2 &= \tilde{e}_2/|\tilde{e}_2| \\ e_3 &= e_1 \times e_2 \end{aligned} \tag{24}$$

and the corresponding orthogonal transformation in $\mathbb{R}^3$

$$O(r_1,r_2) = (e_1^T, e_2^T, e_3^T) \tag{25}$$

The algorithm starts with orienting all the reference configurations ($\alpha = 1, ..., L$) in a special way according to the following procedure. For a given reference configuration r_α, we arrange the atomic coordinates such that $|r_{\alpha 1}| = \min_i |r_{\alpha i}|$ and $|r_{\alpha 2}| = \max_i |r_{\alpha i}|$. The cluster is then rotated using

$$O(r_{\alpha 1}, r_{\alpha 2}) r_{\alpha i} \rightarrow r_{\alpha i} \qquad (i = 1, ..., n) \tag{26}$$

To compare a given cluster configuration r with the αth reference configuration r_α, the following steps are implemented.

(1) The atoms in the configuration of question are relabled so that the condition

$$|r_{\alpha i}| - \epsilon < |r_i| < |r_{\alpha i}| + \epsilon \tag{27}$$

is satisfied for the first two atoms ($i = 1, 2$) and some prespecified tolerance ϵ. (Because the choice of (r_1, r_2) may not be unique, the configuration matching procedure may need to be repeated several times starting with step 1 for all choices satisfying eq 27.)

(2) The orthogonal transformation resulting from the vector pair (r_1, r_2) is then applied to all the atomic coordinates according to

$$O(r_1, r_2) r_i \rightarrow r_i \qquad (i = 1, ..., n) \tag{28}$$

The atoms in the rotated configuration are then relabled, so that the condition (27) is satisfied for all the atoms ($i = 1, ..., n$). If the relabling is successful, configuration r_α is assumed to match the configuration of question.

(3) If the above relabling is impossible, step 2 is repeated, starting with rotation of the original configuration r but using the left-handed basis

$$O(r_2, r_1) r_i \rightarrow r_i \qquad (i = 1, ..., n) \tag{29}$$

(4) If relabling with the left-handed basis is not successful, the inversion around the center-of-mass ($r \rightarrow -r$) is implemented using the original configuration. Step 2 (possibly followed by step 3) is then repeated.

(5) If step 4 is unsuccessful, the algorithm returns to step 2 using a new pair of atoms satisfying condition (27).

Iteration following the above scheme proceeds until eq 27 is satisfied for all r_i.

For a successful comparison, to refine the matching of the two configurations, so that condition (6) is also satisfied, the cluster is rotated further around its center of mass:

$$\tilde{r}_i = \begin{pmatrix} 1 & 0 & 0 \\ 0 & \cos(\phi) & -\sin(\phi) \\ 0 & \sin(\phi) & \cos(\phi) \end{pmatrix} \begin{pmatrix} \cos(\theta) & 0 & -\sin(\theta) \\ 0 & 1 & 0 \\ \sin(\theta) & 0 & \cos(\theta) \end{pmatrix} \begin{pmatrix} \cos(\chi) & -\sin(\chi) & 0 \\ \sin(\chi) & \cos(\chi) & 0 \\ 0 & 0 & 1 \end{pmatrix} r_i \qquad (i = 1, ..., n) \tag{30}$$

The unknown rotational angles (ϕ, θ, χ) are found by minimizing the function

$$f(\phi,\theta,\chi) = ||\tilde{\mathbf{r}}^{\mathrm{T}} Q_\alpha||^2 \tag{31}$$

Note, however, that the minimum value of $f(\phi,\theta,\chi)$ should be zero. Due to the condition (27) the angles in question (ϕ, θ, χ) are very small, so the minimum is usually found in a few iterations. The cluster configuration is then set to $\tilde{r}$.

Finally we note that the latter optimization problem can be solved most efficiently using quaternions that allow one to map it exactly to a 4×4 eigenvalue problem. The corresponding procedure is well described in ref 32.

Acknowledgment. This work was supported by the NSF, grant CHE-0414110. We also thank David Wales, Pavel Frantsuzov, and Christian Predescu for many useful discussions. Dario Meluzzi is aknowledged for his major contribution into writing the replica exchage code used in this work.

References and Notes

(1) Frantz, D. D. *J. Chem. Phys.* **2001**, *115*, 6136.
(2) Doye, J. P. K.; Calvo, F. *Phys. Rev. Lett*. **2001**, *86*, 3570; *J. Chem. Phys.* **2002**, *116*, 8307.
(3) Mandelshtam, V. A.; Frantsuzov, P. A. *J. Chem. Phys.* **2006**, *124*, 204511.
(4) Doye, J. P. K.; Wales, D. J.; Berry, R. S. *J. Chem. Phys.* **1995**, *103*, 4234.
(5) Pillardy, J.; Piela, L. *J. Phys. Chem.* **1995**, *99*, 11805.
(6) Doye, J. P. K.; Wales, D. J. *Chem. Phys. Lett*. **1995**, *247*, 339.
(7) Leary, R. H.; Doye, J. P. K. *Phys. Rev. E* **1999**, *60*, R6320.
(8) Doye, J. P. K.; Miller, M. A.; Wales, D. J. *J. Chem. Phys*. **1999**, *110*, 6896.
(9) Calvo, F.; Neirotti, J. P.; Freeman, D. L.; Doll, J. D. *J. Chem. Phys.* **2000**, **112**, 10340; **2000**, **112**, 10350.
(10) Mandelshtam, V. A.; Frantsuzov, P. A.; Calvo, F. *J. Phys. Chem. A* **2006**, *110*, 5326.
(11) Bogdan, T. V.; Wales, D. J.; Calvo, F. *J. Chem. Phys.* **2006**, *124*, 044102.
(12) Brooks, C. L. J., III; Onuchic, N.; Wales, D. J. *Science* **2001**, *293*, 612.
(13) Geyer, C. J. In *Computing Science and Statistics: Proceedings of the 23rd Symposium on the Interface*; Keramidas, E. K., Ed.; Interface Foundation: Fairfax Station, 1991; p 156.
(14) Hukushima, K.; Nemoto, K. *J. Phys. Soc. Jpn.* **1996**, *65*, 1604.
(15) In ref 3 eq 22 appeared with an error.
(16) Noya, E. G.; Doye, J. P. K. *J. Chem. Phys.* **2006**, **124**, 104503.
(17) Predescu, C.; Predescu, M.; Ciobanu, C. V. *J. Chem. Phys.* **2004**, *120*, 4119.
(18) Calvo F.; Doye, J. P. K. *Phys. Rev. E* **2001**, *63*, 010902.
(19) Sugita, Y.; Okamoto, Y. *Chem. Phys. Lett.* **2000**, *329*, 261.
(20) Mitsutake, A.; Sugita, Y.; Okamoto, Y. *J. Chem. Phys.* **2003**, *118*, 6664; **2003**, *118*, 6676.
(21) Faller, R.; Yan, Q.; de Pablo, J. J. *J. Chem. Phys.* **2002**, *116*, 5419.
(22) Mitsutake, A.; Okamoto, Y. *J. Chem. Phys.* **2004**, *121*, 2491.
(23) Berg, B. A.; Neuhaus, T. *Phys. Rev. Lett.* **1992**, *68*, 9.; Berg, B. A.; Celik, T. *Phys. Rev. Lett.* **1992**, *69*, 2292.
(24) Ferrenberg A. M.; Swendsen, R. H. *Phys. Rev. Lett*. **1988**, *61*, 2635; Ferrenberg, A. M.; Swendsen, R. H. *Phys. Rev. Lett*. **1989**, *63*, 1195.
(25) Sugito Y.; Okamoto, Y. *Chem. Phys. Lett.* **2000**, *329*, 261.
(26) Wang F.; Landau, D. P. *Phys. Rev. Lett*. **2001**, *86*, 2050.
(27) Yan Q.; de Pablo, J. J. *J. Chem. Phys.* **1999**, *111*, 9509; Yan, Q.; de Pablo, J. J. *J. Chem. Phys.* **2000**, *113*, 1276.
(28) Sugita, Y.; Kitao, A.; Okamoto, Y. *J. Chem. Phys.* **2000**, *113*, 6042.
(29) Fukunishi, H.; Watanabe, O.; Takada, S. *J. Chem. Phys.* **2002**, *116*, 9058.
(30) Adjanor, C.; Athenes, M.; Calvo, F. *Eur. Phys. J. B* **2006**, *53*, 47.
(31) Theodorou, D. N. *J. Chem. Phys.* **2006**, *124*, 034109. Uhlnerr A.; Theodorou, D. N. *J. Chem. Phys.* **2006**, *125*, 084107.
(32) Nigra, P.; Freeman, D. L.; Doll, J. D. *J. Chem. Phys.* **2005**, **122**, 114113.
(33) Andricioaei, I.; A. F.; Straub, J. E. *J. Chem. Phys.* **2001**, *114*, 6994.
(34) Frantz, D. D.; Freeman, D. L.; Doll, J. D. *J. Chem. Phys.* **1990**, *93*, 2769.
(35) Eckart, C. *Phys. Rev.* **1935**, *47*, 552.
(36) Wales, D. *Mol. Phys.* **1993**, *78*, 151.
(37) Doye, J. P. K.; Miller, M. A.; Wales D. J. *J. Chem. Phys.* **1999**, *110*, 6896.